

STRATOSPHERIC WARMINGS DURING EARLY WINTER
IN THE NORTHERN AND SOUTHERN HEMISPHERES

G. L. Manney¹, W. A. Lahoz², L. S. Elson¹, L. Froidevaux¹,
R. S. Harwood³, A. O'Neill², R. Swinbank⁴, J. W. Waters¹,
R. W. Zurek¹

¹Jet Propulsion Laboratory/California Institute of Technology, Pasadena, USA

²Centre for Global Atmospheric Modelling, Reading, UK

³Edinburgh University, Edinburgh, UK

⁴Meteorological Office, Bracknell, UK

Submitted to

Quarterly Journal of the Royal Meteorological Society

April 1994

Summary.

The effect of early winter stratospheric minor warmings on the development of the polar vortex is discussed, for winters since the launch of the Upper Atmosphere Research Satellite (UARS). The time evolution of the stratospheric circulation is examined using potential vorticity and UARS Microwave Limb Sounder measurements of ozone (O_3) and water vapour (H_2O). Minor warmings in November and December strongly influence the development of the northern hemisphere (NH) polar vortex in the mid-stratosphere, while in the southern hemisphere (SH) the polar vortex is already sufficiently strong by May that their impact is small. In the NH, strong minor warmings in December are associated with PV and H_2O gradients strengthening along the vortex edge and weakening in mid-latitudes. Synoptic maps of PV, O_3 and H_2O show irreversible mixing in mid-latitudes of air drawn off the vortex and air drawn up from low latitudes, resulting in the changes in tracer gradients described above. In the NH, strong minor warmings in December 1991 and December 1992 mainly affected the middle and upper stratosphere; those in December 1993 mainly affected the middle and lower stratosphere, and resulted in a larger increase in temperatures in the lower stratosphere. Smaller minor warmings also occur in the NH, but have little effect on the size and strength of the polar vortex; however, even small increases in lower stratospheric temperatures are frequently enough to raise three temperatures above the threshold for polar stratospheric cloud formation.

1. Introduction

Stratospheric warmings of varying intensity are common throughout the northern hemisphere (NH) winter (e.g., Andrews et al. 1987). Stratospheric warmings during winter (i.e., excluding the springtime final warming) are arbitrarily classified as "major" if, at

10 hPa, the zonal mean wind poleward of 60° latitude reverses sign, and the zonal mean temperature gradient from 60° to the pole reverses (e.g. Andrews et al. 1987); all others are considered “minor”. In early winter in the NH, the intensification of the polar vortex is accompanied by a variety of minor warmings (Baldwin and Holton 1988; O’Neill and Pope 1990). Several studies (Labitzke 1977, Clough et al. 1985, Juckes and O’Neill 1988) described one type, known as Canadian warmings (Labitzke 1977). Farrara et al. (1992) showed that minor warmings are also common during early winter in the southern hemisphere (SH), and that some of these strongly resemble the NH Canadian warmings (these are referred to as South Pacific warmings).

Canadian or South Pacific type warmings exhibit the following characteristics:

- The cyclonic vortex remains strong, while being displaced from the pole; in a wavenumber decomposition, this appears as a circulation dominated by a wave 1 pattern,
- The flow is affected mainly in the middle and lower stratosphere, and the disturbance is nearly equivalent barotropic, i.e., it shows little or no longitudinal phase tilt with height.
- The disturbance moves slowly eastward.

Juckes and O’Neill (1988) show evidence that Canadian warmings may be a stratospheric response to the establishment in the troposphere of the climatological east Asian low. Juckes and O’Neill (1988) and Baldwin and Holton (1988) suggest that Canadian warmings are involved in the formation of the main vortex/surf zone structure (McIntyre and Palmer 1984), as changes in the distribution of potential vorticity result from nonconservative effects of radiation acting on a disturbed circulation, and from PV being drawn out into long tongues during the warming that eventually become too narrow to be resolved.

in the following, we examine minor warmings in early winter since the launch of the Upper Atmosphere Research Satellite (UARS) in September 1991. We are interested in the vertical extent and structure of early winter warmings, and their effect on the

development of the polar vortex; a related question is the effect of these disturbances on transport. We examine ozone (O_3) and water vapour (H_2O) data from the Microwave Limb Sounder (MLS) instrument on UARS to investigate the effect of these warmings on their distribution and their relation to the polar vortex.

2. Data and Analysis

The meteorological data (horizontal winds, geopotential heights and temperatures) are analyses from the United Kingdom Meteorological Office (UKMO) assimilation system (Swinbank and O'Neil, 1994) that was developed for the UARS project. The Rossby-Ertel potential vorticity (PV) is calculated from these employing the algorithm described by Manney and Zurek (1993),

The MLS O_3 data used here are from the 205 GHz radiometer; the H_2O data are from the 183 GHz radiometer. The UARS MLS instrument is described by Barath et al. (1993). The MLS data have a horizontal resolution of approximately 400 km and a vertical resolution of approximately 4 km. Some aspects of the O_3 data and retrievals are described by Froidevaux et al. (1994), and of the H_2O data by Lahoz et al. (1994). Root-mean-square (rms) precision of individual O_3 measurements between 50 hPa and 1 hPa are ≈ 0.3 ppmv, with absolute accuracies of $\approx 5-10\%$ in the middle and upper stratosphere, and 10-30% in the lower stratosphere (Froidevaux et al. 1994, paper in preparation). Single profile precision and accuracy estimates for H_2O are 0.3 ppmv and 15% at 4.6 hPa (Lahoz et al. 1994, paper in preparation). Between ≈ 20 hPa and 50 hPa, H_2O data quality is generally good only at low and middle latitudes. At high latitudes in winter, the 1120 data may have a substantial component from climatology at 50 hPa (Lahoz et al. 1994, paper in preparation). H_2O data are shown only from approximately 20 hPa to approximately 1 hPa here. MLS data are gridded using Fourier transform techniques that separate time and longitude variations (Elson and Froidevaux 1993). Since MLS

temperatures are currently available only for pressures ≤ 22 hPa, UK MO temperatures are used to interpolate gridded MLS data to isentropic surfaces.

We examine the stratospheric flow during November and December 1991, 1992, and 1993 in the NH, and during May and June 1992 and 1993 in the SH. Since the MIS instrument switches approximately every 36 days from observing 34°S to 80°N to observing 80°S to 34°N , we have available MLS observations in the hemisphere of interest during approximately the second half of each of the periods studied. MLS data for the S11 in June 1992 are limited, due to a spacecraft anomaly (Reber 1993). The 183 GHz radiometer on the MLS failed in late April 1993, so no stratospheric 11_2 data are available after that time.

3. Overview of Early Winter Warmings

Figure 1 shows time series for each of the early winter periods of zonal mean winds and temperatures, and the zonal wavenumber 1 (wave 1) and zonal wavenumber 2 (wave 2) components of the geopotential height field, at 10 hPa in the mid-stratosphere. The wave 1 and wave 2 time series have phase (longitude of one maximum) at 60° latitude superimposed. The build-up of the polar vortex is evident in the overall strengthening of the westerlies and decrease in temperatures throughout the time period (the exception is at the end of December 1993, when a major stratospheric warming is beginning, halting the strengthening of the polar vortex). The build up of the vortex is by no means monotonic, particularly in the NH. As is well known (e.g., Andrews 1989, Manney and Zurek 1993), the polar vortex develops much more quickly and monotonically in the S11 than in the NH. The approximate times of the more noticeable early winter minor warmings are indicated on the plots of zonal mean wind. We see events having a wide variety of impact on the zonal mean winds and temperatures, and much interannual variability in both hemispheres. Strong minor warmings occur in December for each of the three NH I

winters shown. in the SH, there are more frequent warmings in 1992 than in 1993, although their net effect on the build-up of the strong SI 1 polar vortex is small in each year, as evidenced by the very strong westerlies and cold temperatures that have developed by the end of June.

The time series of wave 1 and wave 2 show that the disturbances to the flow are usually dominated by the wave I component, i.e., the cyclonic vortex is shifted off the pole. In the NH, this shift represents the build up of the Aleutian anticyclone centered at $\approx 180^\circ$, as described by Jukes and O'Neill (1988). in the SH, the polar vortex generally shifts towards South America, so an anticyclone develops over the South Pacific, as noted by Farrara et al (1992). There is, however, considerably more variability in vortex position in the SH early winter than in the NH, and the SH anticyclone is a transient feature. Although this shift off the pole is the most obvious feature, there is frequently a considerable, amplification of wave 2 associated with these warmings, representing an elongation of the polar vortex, particularly in the NH (e.g., late November 1992 and late November 1993). The phase shown in these plots suggests a slow eastward rotation associated with some, but not all, of the early winter warmings, with more eastward motion apparent in the SH. The wavenumber decomposition also reflects the large degree of interannual variability of these events in both hemispheres. The maximum wave amplitudes reach somewhat higher values during the strongest events in the NH. There are, however, winters (e.g., compare 1992 in the NH with the two SH winters shown) where the wave amplitudes in the SH are as large or larger than those in the NH. As is apparent in the zonal mean winds, and as noted by Manney and Zurek (1993), by the beginning of May, the SH polar vortex has already strengthened much further than the NH vortex at the beginning of November. Thus, against the background of a stronger polar vortex, the disturbances have less impact. The zonal mean/wavenumber decomposition is also less representative of the processes occurring in the NH since the flow is more distorted there (e.g., Jukes and O'Neill 1988).

Figure 2 shows the vertical structure of the warmings as a function of time. The maximum amplitude of the geopotential height field with the zonal mean removed at each altitude (i. e., $\max[|Z - \bar{Z}|]$), is plotted as a function of pressure and time at 64° latitude, near the latitude where wave amplitudes are largest. Wave amplitudes are often strongest in the upper stratosphere at or above 1 hPa, i.e., during November 1991, 1992 and 1993, December 1991 and 1992, and May 1992. A few of these events that are strongest in the upper stratosphere show significant amplitudes extending into the lower stratosphere, those with peak amplitudes on about 20 Nov 1991, 20 Dec 1991, and 10 Dec 1992. A few disturbances have largest wave amplitudes in the mid-stratosphere, between 10 and 2 hPa in the NH and 20 and 5 hPa in the SH, for instance, on about 14 Dec 1993, 15 Jun 1992 and 18 Jun 1992; these in general extend into the lower stratosphere. None of the events shows more than about two days delay in amplification in the lower stratosphere after the upper stratospheric amplification; those that are largest in the mid-stratosphere appear to amplify nearly simultaneously at all levels,

Figure 3 shows time series for the same periods of minimum high latitude temperatures in the lower stratosphere at 520 K (≈ 40 hPa). The uncertainty in the individual temperature values given here is approximately 2 K (Swinbank and O'Neil 1994). Lower stratospheric temperatures are of particular interest since they determine whether conditions are favorable for the formation of polar stratospheric clouds (PSCs). The threshold for formation of type 1 PSCs is about 195 K in the lower stratosphere. In the SH, temperatures descend below the PSC formation threshold in early May, and continue to decrease dramatically. Those warmings that extend into the lower stratosphere are accompanied by an increase in temperatures for a few days, followed by a return to the overall decreasing trend; these SH events do not have a significant impact on the likelihood or timing of PSC formation. In contrast, the warmings are more sustained in the NH, and temperatures are initially higher. Again, those events that extend into the lower stratosphere are accompanied by an increase in temperatures; the most dramatic such occurrence is on

about **14 Dec 1993. However**, with the warmer NH temperatures and more sustained disturbances, even the smaller warmings cause lower stratospheric temperatures to fluctuate around the threshold for PSC formation, varying from about 5 K above to about 5 K below this threshold. Thus the pattern of early winter minor warmings in a given year in the NH strongly impacts the development of conditions favorable to PSC formation, chlorine activation and chemical depletion of O_3 .

Figure 4 shows the vertical synoptic structure of the disturbances. For each event marked in Fig. 1, the geopotential height field, minus the zonal mean, is shown as a function of longitude and pressure averaged over 60° to 68° latitude, similar to figures shown by Farrara et al. (1992). Each of these is for a day closely preceding the peak of the warming. Again, a good deal of variation is seen in the structure of the disturbance during different events. The majority of the fields show nearly equivalent barotropic structure, with little phase tilt with height, in common with Canadian or South Pacific type warmings. However, several events (i.e., 4 Nov 1991, 4 Nov 1992, 10 Dec 1992, and 30 Nov 1993) show a considerable westward tilt with height, a characteristic frequently seen in strong mid- and late-winter warmings in the NH (Fairlie et al. 1990; Manney et al. 1994a,b; Lahoz et al. 1994). The degree of phase tilt does not appear to be related closely to the altitude of maximum amplitude in that there are examples of warmings that peak in the upper stratosphere and in the mid-stratosphere with both significant and insignificant phase tilts with height. The warmings around 14 Dec 1993, 15 Jun 1992 and 18 Jun 1993 most closely resemble Canadian or South Pacific warmings, in that maximum amplitudes are in the mid-stratosphere, they show little phase tilt with height, and there is some eastward motion of the disturbance (Fig. 1).

Figure 5 shows the 840 K (≈ 10 hPa) PV field for each event on the same days as in Fig. 4. The greater impact of the disturbances on the weaker NH vortex is immediately apparent. Considerable elongation of the vortex is seen on 26 Nov 1992 and 30 Nov 1993, corresponding to the large wave 2 amplitudes shown in Fig. 1. Although, as shown

in Fig. 1, the vortex occasionally rotates eastward during the warmings, most show the vortex shifted off the pole towards 0° longitude, and the anticyclone forming near 180° . Most of the warmings in the NH show air from low latitudes being pulled into the polar regions between the cyclone and anticyclone, and tongues of high PV being stripped off the edge of the vortex. Similar behavior can be seen in the relatively strong warming around 18 Jun 1993 in the SH.

4. Evolution of potential vorticity and trace species

We examine here the day to day evolution of the stratospheric flow and available MLS trace species (O_3 , H_2O) data during some of the more prominent warmings in December 1992, December 1993, and June 1993. H_2O generally behaves as a passive tracer through most of the stratosphere (e.g., Brasseur and Solomon 1984); chemical time constants for O_3 vary strongly with latitude and season in the middle and upper stratosphere, with O_3 being produced in low latitudes in the mid-stratosphere (e.g., Brasseur and Solomon 1984); in high latitudes in winter chemical time constants for O_3 are long compared to dynamical time scales at all altitudes shown here (e.g., Garcia and Solomon 1985).

Figure 6 shows a sequence of maps at 840 K of H_2O and O_3 mixing ratios, with several PV contours overlaid, for 30 Nov 1992 through 16 Dec 1992, and 22 through 26 Dec 1992, when MLS was viewing high northern latitudes in early winter 1992. The PV contours shown are in the region of strong gradients (compare with Fig. 5) along the polar night jet core which can be used to demarcate the edge of the polar vortex. Eastward rotation of the vortex is apparent between 30 Nov and 6 Dec, and again starting on 14 Dec 1992, with the vortex stationary between those times. Throughout this time period, a prominent feature of the flow is the tongues of high PV air being drawn off the edge of the vortex, and low PV air being drawn into high latitudes in the region of the

anticyclone. Tongues of high H_2O being peeled off the vortex edge, and low H_2O being drawn in from low latitudes are well correlated with PV. Similar features are seen in the O_3 fields, although the horizontal gradients of O_3 mixing ratio are not as strong as those of H_2O in the region near the edge of the vortex. During 30 November through 8 December, high O_3 from low latitudes can be seen moving into the region of the anticyclone. Evidence can also be seen during this time of low O_3 being drawn off the edge of the vortex. After about 12 December, a patch of low O_3 forms in the anticyclone; chemical effects are thought to be important in the formation of this low O_3 anomaly (Manney et al., paper in preparation). The likely influence of chemistry in middle and low latitudes complicates interpretation of the evolution of O_3 , but strong correlations between the behavior of PV, O_3 and H_2O are apparent everywhere through about 10 December, and throughout the time period shown in high latitudes.

Figure 7 shows the evolution of O_3 and PV in December 1993. Slow eastward rotation of the vortex is apparent throughout the time period. Again, tongues of high PV/low O_3 air are drawn off the edge of the vortex, and low PV/high O_3 air is drawn from low latitudes into the region of the anticyclone, and a low ozone anomaly again develops.

Figure 8 shows the evolution of O_3 and PV during a minor warming in the SH in late June 1993. More rapid eastward rotation of the vortex is apparent than in the NH cases shown above; if sustained, the eastward motion in this case would correspond to a period of about 8 to 16 days, whereas the rotation in Figs. 6 and 7 in the NH would correspond to periods of about 20 to 40 days. The vortex in June in the SH is larger and stronger than that in December in the NH, so the impact of the warming on its evolution is smaller. However, there is still evidence of high PV/low O_3 air being drawn in a tongue off the edge of the vortex in the SH, and the map on 20 June suggests that high O_3 from low latitudes is being moved into higher latitudes.

Area integrals of PV (Butchart and Remsberg 1986) at 520 K (≈ 40 hPa), 655 K (≈ 20 hPa), 840 K (≈ 10 hPa) and 1000 K (≈ 5 hPa) show the evolution of the polar vortex during

the times studied here (Figure 9). A common feature of the three NH early winters is the development of a main vortex/surf zone structure in early December, as PV gradients increase, along the edge of the vortex and decrease in mid-latitudes. In 1991 and 1992 in the NH, the strongest warmings in December affected mainly the middle and upper stratosphere while in 1993 the strongest warmings (prior to the major warming at the end of December) affected mainly the middle and lower stratosphere. In mid-December 1991 and 1992 at 840 and 1100 K, PV gradients along the vortex edge (near 60° equivalent latitude) steepen rapidly leading to a pattern with very steep gradients along the vortex edge and weak gradients in low latitudes. These changes are coincident with the onset of strong warmings. Only a very small change associated with the warmings is seen at 655 K in 1991 and 1992, and the development at 520 K proceeds at a steady rate, with little effect of warmings apparent. In contrast, in 1993, when the strongest warmings affect mainly the mid-stratosphere, a smaller effect is seen at 1100 K, and a larger one at 655 K. In late November 1993, PV gradients weaken and vortex area shrinks for about 10 days, followed by rapid strengthening of high latitude and weakening of mid-latitude gradients. This behavior is also apparent to a lesser degree at 520 K. Early December 1993 is the time when lower stratospheric temperatures are most strongly affected by the warmings (Fig. 3c). In late December 1992, PV gradients decreased slightly at the vortex edge, and the size of the vortex decreases slightly. The times when vortex area decreases are also times when the disturbance to the flow shows significant phase tilt with height,

in the SH, the vortex is already sufficiently strong by May that any effect of the warmings is difficult to detect. In each of the two years shown here, a relatively strong warming occurred in the latter half of June. In both years, a slight strengthening of PV gradients along the vortex edge can be seen in the 840 and 655 K plots. Comparing with the NH, we see that, although the vortex is larger and stronger in the SH, at the end of the periods shown here, the PV gradients in mid-latitudes are stronger in the SH than in the NH, especially at 840 and 1100 K. A small effect is also seen on about 20 May 1992 at

each level. A significant increase in lower stratospheric temperatures occurs at the same time (Fig. 3d).

Figure 10 shows similar area integrals of H_2O mixing ratio for December 1992 (the time period shown is marked in Figure 9) at 1100, 840, and 655 K. The behavior of H_2O is similar to that of PV; a slight strengthening of gradients is seen along the vortex edge and a substantial weakening of gradients in mid-latitudes. This is consistent with the behavior expected when tongues of high H_2O are drawn off the edge of the vortex, and mix in mid-latitudes, as was shown in Figure 6. As with the PV contours in 1992, the changes in H_2O are most prominent at 1100 and 840 K, and weaker at 655 K.

Figure 11 shows overall changes in H_2O and O_3 for December 1992, and in O_3 for December 1993 and June 1993. Cross-sections are shown as a function of θ and latitude along a meridian from equator to pole to equator, through the polar vortex, near the beginning and end of the period when MIS was observing the appropriate hemisphere. Between the end of November 1992 and the beginning of January 1993, the contours between 5.0 and 6.2 ppmv (yellow-green colours) shown in the H_2O field have shifted downward in the region poleward of about 30°N by between 50 and 200 K, suggesting diabatic descent rates ($d\theta/dt$) over the period of as much as 7 K d^{-1} at some places in the middle to upper stratosphere. Examining those same contours, we also see in the H_2O plot for 3 Jan 1993 a more pronounced pattern of strong horizontal gradients (i.e., vertical contours) in low latitudes and at the edge of the vortex, and weak horizontal gradients in between; this pattern is prominent along 180° longitude. This is reminiscent of the surf zone/main vortex structure. The pattern of descent seen here is very similar to that shown by Lahoz et al. (1994) during a strong warming in January 1992. Higher H_2O mixing ratios extend to lower altitudes along 180° longitude on 30 Nov 1992 near 35°N , and along 0° longitude near 30°N on 3 Jan 1993; the cross-sections here cut across tongues of high water that have been pulled off the edge of the vortex (the tongue on 30 Nov 1992 can be seen in Fig. 6). On 30 Nov 1992, there is also apparent a region of lower H_2O that

has been drawn in from low latitudes. These cross-sections indicate that tongues of air pulled off the vortex may be quite deep.

in O_3 for the same time period we can see the effects of descent in the vortex, where O_3 has increased substantially below the O_3 peak. O_3 increases in the lower stratosphere extend from the pole to outside the edge of the vortex, suggesting that descent is important throughout that region. As previously noted (e.g., Jukes and O'Neill 1988), diabatic descent is enhanced during stratospheric warmings. High latitude O_3 in fact increases throughout the altitude region shown here during December 1992. This suggests that horizontal poleward transport is more important in changing O_3 than diabatic descent at levels above the O_3 peak. It is difficult to relate other changes in mid and low latitude O_3 in the middle and upper stratosphere to transport since, as discussed above, some of the changes in the middle and upper stratosphere are due to chemical mechanisms.

The O_3 fields for late November and late December 1993 show a similar pattern, with O_3 increasing inside the vortex below the O_3 peak, and the O_3 increase in the lower stratosphere extending outside the vortex; however, in December 1993, ozone in the vortex above the peak decreases. As noted earlier, the warmings during December 1993 affected mainly the middle and lower stratosphere, while those in December 1992 affected mainly the middle and upper stratosphere. This is consistent with the cross-sections which suggest that horizontal transport in the upper stratosphere is less important in December 1993 than in December 1992. The increase in ozone in the middle and lower stratospheric vortex appears somewhat greater in December 1993 than in December 1992, consistent with a greater effect of the warmings at those levels in 1993, and with additional enhancement of descent associated with the beginning of a virtually major stratospheric warming at the end of December 1993.

A pattern qualitatively very similar to that in December 1993 in the NH is seen in the SH between the beginning of June and the beginning of July 1993. Ozone increases in the vortex below the peak, and decreases above. The ozone increase in the lower

stratosphere appears to extend further equatorward from the vortex in the SH than in the NH. Although a quantitative estimate is beyond the scope of this paper, the increase in O_3 mixing ratio below the ozone peak is considerably less in the SH than in the NH. This suggests more descent in the NH than in the SH, as would be expected from higher NH temperatures and stronger and more sustained N_1 warmings.

5. Discussion and Conclusions

We have examined the effect of minor warmings on the evolution of the stratospheric circulation in early winter in both northern and southern hemispheres, for several winters since the launch of UARS. The evolution of O_3 and H_2O , measured by the UARS MLS is examined to aid in interpreting the effects of these warmings.

Minor warmings are common in both NH and SH early winters, and have a wide variety of characteristics. Examples are shown of warmings which affect mainly the middle and upper stratosphere and ones that affect mainly the middle and lower stratosphere. While many events are nearly equivalent barotropic, others show considerable westward phase tilt with height. Most early winter minor warmings consist mainly of a displacement of the vortex off the pole (i.e., wave 1 is large); however, there are also events where the vortex is considerably elongated (i.e., wave 2 is large). Minor warmings in the NH early winter produce large decreases in zonal mean winds and increases in zonal mean temperatures. In contrast, although disturbance amplitudes can be as large in the SH as in the NH, the SH polar vortex is sufficiently strong by May that the impact of these events is small.

The synoptic evolution in the NH mid-stratosphere shows tongues of high PV, high H_2O and low O_3 being drawn off the edge of the vortex during the warmings and irreversibly mixed in mid-latitudes. Tongues of low PV, low H_2O and high O_3 are also drawn into the region of the anticyclone from low latitudes. This behavior results in a

strengthening of PV and trace species gradients along the edge of the polar vortex, and weakening, of gradients in mid-latitudes. This formation in the NH of this main vortex/surf zone type structure is coincident with the onset of strong minor warmings, and the episodic nature of its development suggests, as has been previously discussed (Clough et al. 1985, Jukes and O'Neil 1988), that minor stratospheric warmings during early winter are instrumental in the formation of this structure. Although tongues of material can be seen being drawn off the edge of the SH polar vortex during early winter minor warmings, only a slight tendency for PV gradients to increase along the edge of the vortex and decrease outside is noted during the SH warmings. The main vortex/surf zone type structure thus never becomes as prominent in the SH as in the NH.

The meteorological and satellite data studied here provide a coarse-grain picture of these events due to their low horizontal resolution (e.g., Clough et al. 1985). High-resolution modelling techniques such as contour advection (e.g., Waugh et al. 1994) and domain-filling trajectory calculations (e.g., Sutton et al. 1994) will eventually provide further insight into the fate of tongues of air drawn off the vortex after they become too narrow to be resolved by the UARS measurements. This is of relevance to determining the degree of mixing between polar and mid-latitude air, and how much this mixing is enhanced by warming events such as those discussed here.

Evidence of enhanced diabatic descent at middle and high latitudes during the warmings is seen in vertical sections of H_2O and O_3 . Comparison of vertical sections of O_3 during NH and SH warmings shows stronger diabatic descent in the NH, where temperatures are higher and the warmings are more sustained.

In the SH, the polar vortex is sufficiently strong in May and June that the early winter minor warmings have little impact on its development. In contrast, the timing, vertical structure and intensity of stratospheric warmings during early winter have a profound impact on vortex development in the NH, and consequently on lower stratospheric temperatures there. During December in the NH, lower stratospheric temperatures are

generally near the threshold for PSC formation; even weak minor warmings that influence the middle and lower stratosphere may cause temperatures to fluctuate above and below this threshold, and thus affect the timing and frequency of occurrence of PSCs. In addition, the patterns of wave activity in early winter and their effect on the lower stratospheric vortex strongly influence the strength of the lower stratospheric vortex for the remainder of the winter (Zurek et al. 1994, paper in preparation). As shown here, these events exhibit a large degree of interannual variability.

Acknowledgments. Thanks to our MLS colleagues for their contributions to its success; to T. Luu for data management and graphics, to P. Newman for supplying routines that were adapted to calculate PV. The UARS investigations at JPL/CalTech were carried out under contract with NASA.

References

- Andrews, D. G., J. R. Holton, and C. B. Leovy, 1987: *Middle Atmosphere Dynamics*. Academic Press, New York, 489pp.
- Andrews, D. G., 1989: Some comparisons between the middle atmosphere dynamics of the southern and northern hemispheres. *PAGEOPH*, **130**, 213-232.
- Baldwin, M. P., and J. R. Holton, 1988: Climatology of the stratospheric polar vortex and planetary wave breaking, *J. Atmos. Sci.*, **45**, 1123-1142.
- Barath, F. T., M. C. Chavez, R. E. Cofield, D. A. Flower, M. A. Frerking, M. B. Gram, W. M. Harris, J. R. Holden, R. F. Jarnot, W. G. Kloezen, G. J. Klose, G. K. Lau, M. S. 1.00, B. J. Maddison, R. J. Mattauch, R. P. McKinney, G. E. Peckham, H. M. Pickett, G. Siebes, F. S. Soltis, R. A. Suttie, J. A. Tarsala, J. W. Waters, and W. J. Wilson, 1993: The Upper Atmosphere Research Satellite Microwave Limb Sounder instrument, *J. Geophys. Res.*, **98**, 1 (1,751 -10,762).
- Brasseur, G., and S. Solomon, 1984: *Aeronomy of the Middle Atmosphere*. Reidel, Dordrecht, 441 pp.
- Clough, S. A., N. S. Grahame, and A. O'Neill, 1985: Potential vorticity in the stratosphere derived using data from satellites, *Q. J. Roy. Meteor. Soc.*, **111**, 33 S-358.
- Dunkerton, T. J., and D. P. Delisi, 1986: Evolution of potential vorticity in the winter stratosphere of January-February, 1979. *J. Geophys. Res.*, **91**, 1 199-1208.
- Elson, L. S., and L. Froidevaux, 1993: The use of Fourier transforms for synoptic mapping: Early results from the Upper Atmosphere research Satellite Microwave Limb Sounder, *J. Geophys. Res.*, **98**, 23,039-23,049.
- Fairlie, T. D. A., M. Fisher, and A. O'Neill, 1990: The development of narrow baroclinic zones and other small-scale structure in the stratosphere during simulated major warmings. *Quart. J. Roy. Meteor. Soc.*, **116**, 287-315.
-

- Farrara, J. D., M. Fisher, C. R. Mechoso, and A. O'Neill, 1992: Planetary-scale disturbances in the southern stratosphere during early winter. *J. Atmos. Sci.*, **49**, 1757-1775.
- Froidevaux, L., J. W. Waters, W. G. Read, L. S. Elson, D. A. Flower, and R. F. Jarnot, 1994: Global O₃ observations from UARS MLS: An overview of zonal mean results. *J. Atmos. Sci.*, submitted.
- Garcia, R. R., and S. Solomon, 1985: The effect of breaking gravity waves on the dynamics and chemical composition of the mesosphere and lower thermosphere. *J. Geophys. Res.*, **90**, 3850-3868.
- Juckes, M. N., and A. O'Neill, 1988: Early winter in the northern hemisphere. *Quart. J. Roy. Meteor. Soc.*, **114**, 1111-1125.
- Labitzke, K., 1977: Interannual variability of the winter stratosphere of the northern hemisphere. *Mon. Wea. Rev.*, **105**, 762-770.
- Lahoz, W. A., A. O'Neill, E. S. Carr, R. S. Harwood, L. Froidevaux, W. G. Read, J. W. Waters, J. B. Kumer, J. L. Mergenthaler, A. E. Roche, G. E. Peckham, and R. Swinbank, 1994: Three-dimensional evolution of water vapour distributions in the northern hemisphere as observed by MLS. *J. Atmos. Sci.*, submitted.
- Manney, G. L., and R. W. Zurek, 1993: Interhemispheric comparison of the development of the stratospheric polar vortex during fall: A 3-dimensional perspective for 1991-1992. *Geophys. Res. Lett.*, **20**, 1275-1278.
- Manney, G. L., J. D. Farrara, and C. R. Mechoso, 1994a: Simulations of the February 1979 stratospheric sudden warming: Model comparisons and Three-dimensional evolution, *Mon. Wea. Rev.*, **122**, 1115-1140.
- Manney, G. L., R. W. Zurek, A. O'Neill, R. Swinbank, J. B. Kumer, J. L. Mergenthaler, and A. E. Roche, 1994b: Stratospheric Warmings during February and March 1993. *Geophys. Res. Lett.*, in press.

Figure Captions

Figure 1. Time series at 10 hPa of zonal mean wind, zonal mean temperature, and wavenumber 1 and 2 components of the geopotential height field, for five early winters. The time period in the NH is from 1 November to 3 January, in the SH from 1 May to 3 July. Zonal mean wind contours are every 10 m s^{-1} , with 40 to 50 m s^{-1} shaded. Zonal mean temperature contours are every 2.5 K, with 212.5 to 215 K shaded. Wave 1 and wave 2 contours are every 100 m, with 800 to 900 m shaded for wave 1 and 400 to 500 m shaded for wave 2. The black dots on the wave 1 and wave 2 plots show the phase (longitude of one maximum) at 60° latitude. The black triangles at the bottom of the zonal mean wind plots show the approximate times of early winter warmings to be discussed here.

Figure 2. Time series at 64° latitude (north or south) of the maximum amplitude of the geopotential height field with the zonal mean removed, i.e., $\max[|Z(\lambda, 64^\circ) - \bar{Z}(64^\circ)|]$, where λ is longitude, and \bar{Z} is the zonal mean geopotential height. Time series are for the same periods shown in Figure 1. Contour interval is 100 m, with 1100 to 1200 m shaded.

Figure 3. Time series for the five winters of minimum temperatures on the 520 K isentropic surface, in the region where potential vorticity (PV) is greater than $0.4 \times 10^{-4} \text{ K m}^2 \text{ kg}^{-1} \text{ s}^{-1}$. The thin horizontal line is at 195 K, an approximation to the threshold temperature for the formation of polar stratospheric clouds.

Figure 4. Longitude-pressure cross-sections of the geopotential height with the zonal mean removed, averaged over 60 to 68° latitude, on a day near the peak of each of the warmings indicated in Figure 1,

Figure 5. Rossby-Ertel potential vorticity (PV) on the 840 K isentropic surface, with wind vectors superimposed, for the same days shown in Figure 4. The contour interval is $1.0 \times 10^{-4} \text{ K m}^2 \text{ kg}^{-1} \text{ s}^{-1}$, with 4 to $5 \times 10^{-4} \text{ K m}^2 \text{ kg}^{-1} \text{ s}^{-1}$ shaded. The

- McIntyre, M. E., and T. N. Palmer, 1984: The 'surf zone' in the stratosphere, *J. Atmos. Terr. Phys.*, 46, 825-849.
- O'Neill, A., and V. D. Pope, 1990: The seasonal evolution of the extra-tropical stratosphere in the southern and northern hemispheres: Systematic changes in potential vorticity and the non-conservative effects of radiation, Dynamics, *Transport and Photochemistry in the Middle Atmosphere of the Southern Hemisphere*, 33-54, Kluwer Academic Publishers, Netherlands.
- Reber, C. A., 1993: The Upper Atmosphere Research Satellite (UARS). *Geophys. Res. Lett.*, 20, 1215-1218.
- Sutton, R., and H. MacLean, 1994: High resolution middle atmosphere tracer fields estimated from satellite observations using Lagrangian trajectory calculations. *J. Atmos. Sci.*, submitted.
- Swinbank, R., and A. O'Neill, 1994: A Stratosphere-troposphere data assimilation system. *Mon. Wea. Rev.*, **122**, 686-702.
- Waugh, D. W., R. A. Plumb, R. J. Atkinson, M. R. Schoeberl, L. R. Lait, P. A. Newman, M. Loewenstein, D. W. Toohey, L. M. Avallone, C. R. Webster, and R. D. May, 1994: Transport out of the lower stratospheric Arctic vortex by Rossby wave breaking, *J. Geophys. Res.*, 99, 1071-1088,

projection is orthographic, with 0° longitude at the bottom of the NH plots and at the top of the SH plots, and 90°E to the right. 300° and 60° latitudes are shown as fine dashed lines.

Figure 6, Synoptic maps of water vapour (H_2O) and ozone (O_3), with overlaid PV contours on the 840 K isentropic surface, for days in the NH early winter of 1992. The PV contours shown are 2, 3, 4, 5, and $6 \times 10^{-4} \text{ K m}^2 \text{ kg}^{-1} \text{ s}^{-1}$. The layout of the plots is the same as in Figure. 5.

Figure 7. As in Figure 6, but for O_3 only, in the NH 1993 early winter.

Figure 8. As in Figure 7, but for the SH 1993 early winter.

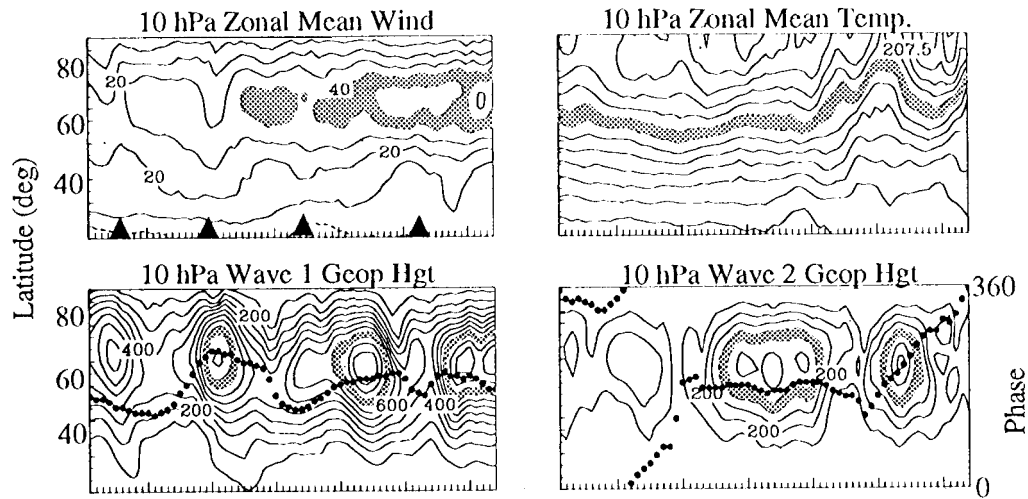
Figure 9. Time series of area integrals of PV for the five early winters, on the 1100 K, 840 K, 655 K, and 520 K isentropic surfaces, running from 1 November (1 May) to 3 January (3 July) in the NH (SH). Area is expressed in terms of equivalent latitude. PV was scaled in "vorticity units" (Dunkerton and Delisi 1986, Manney and Zurek 1993) by dividing by a standard atmosphere value of the static stability, so that the numbers have a similar range at each level. In these units, the contours run from 0.8 to $3.0 \times 10^{-4} \text{ s}^{-1}$, with a contour interval of $0.2 \times 10^{-4} \text{ s}^{-1}$. The discontinuity in the NH plots for 1991 on about 5 December is due to changes in the processing of UKMO data made at this time (Swinbank and O'Neil 1994). The heavy vertical lines on the NH 1992 plots show the beginning of the time period shown in Figure 10.

Figure 10. Area integrals similar to Figure 9, but of H_2O mixing ratio, from 30 November through 3 January 1992 in the NH, at 1100 K, 840 K, and 655 K. The contours at 1100 K are from 6.0 to 7.1 ppmv, with a contour interval of 0.1 ppmv. The contours at 840 K are from 5.0 to 6.65 ppmv, with a contour interval of 0.15 ppmv. The contours at 655 K are from 4.6 to 5.7 ppmv, with a contour interval of 0.1 ppmv.

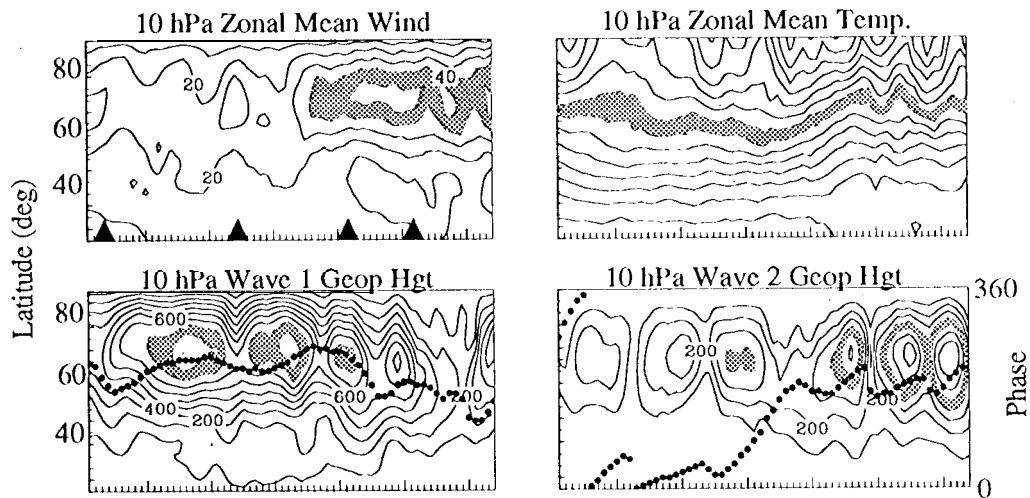
Figure 11. Cross-sections from equator to pole to equator as a function of potential temperature (θ), of (a) and (b) H_2O and (c) through (h) O_3 mixing ratios (ppmv) on days

near the beginning and the end of observing periods in (a) through (d) NH early winter 1992, (e) and (f) NH early winter 1993, and (g) and (h) SH early winter 1993. (a) through (d) and (g) and (h) are along 0° to 180° longitude. (e) and (f) are along 90° to 270° longitude. The thin black lines show the $1.4 \times 10^{-4} \text{ s}^{-1}$ contour of PV scaled in "vorticity units", a value that is within the region of strong PV gradients at all levels shown here (see Fig. 9).

1991-1992



1992-1993



1993-1994

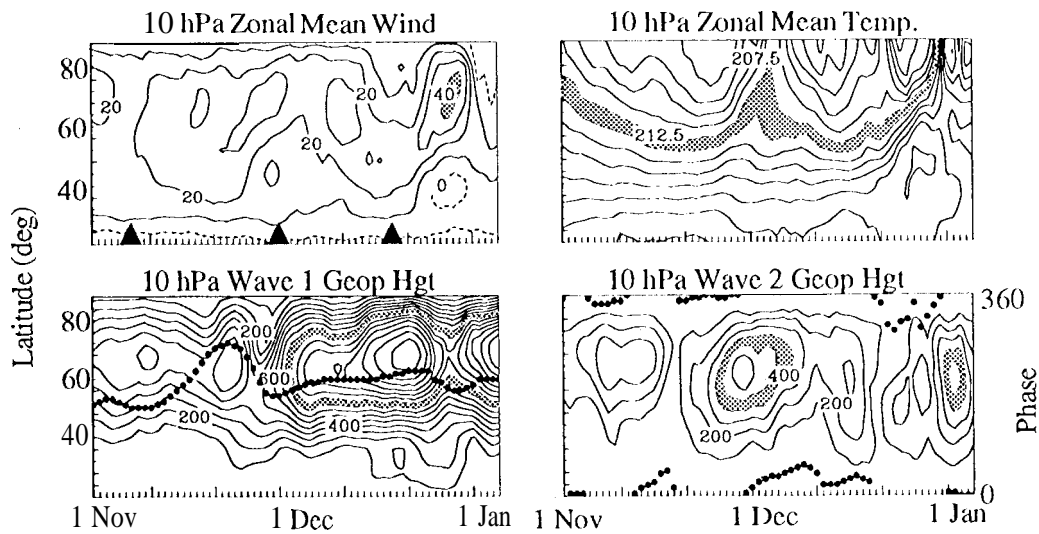
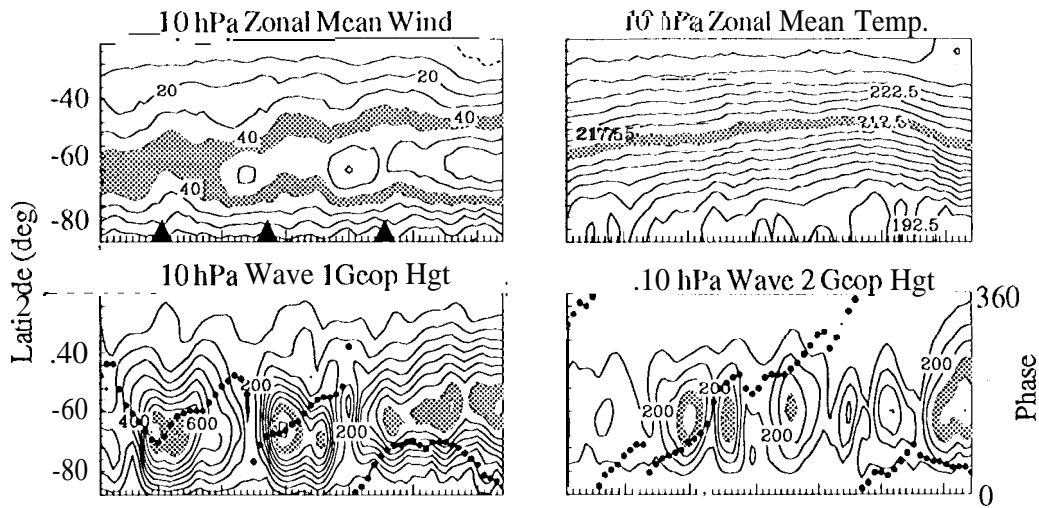


Fig. 1

1992



1993

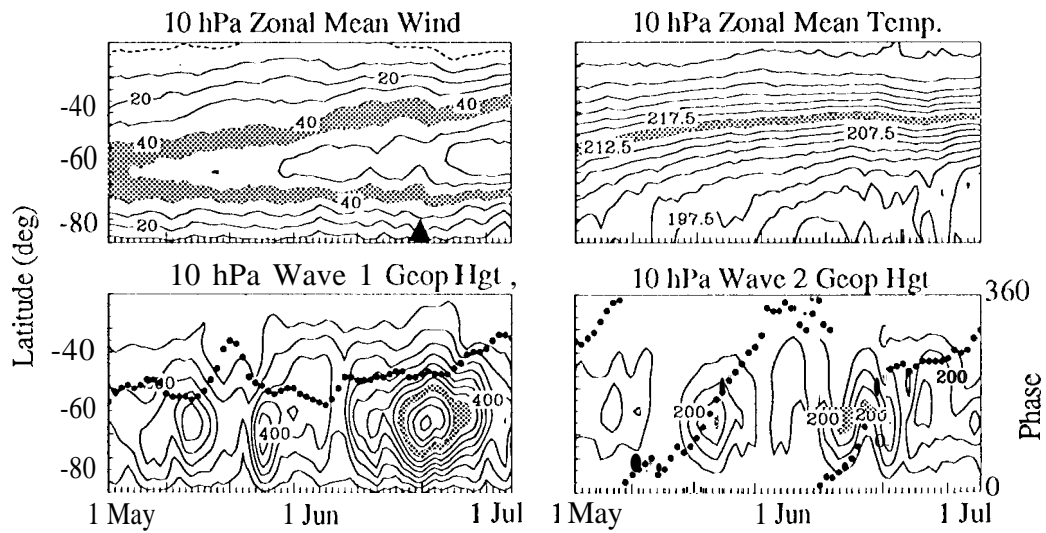


Fig. 1

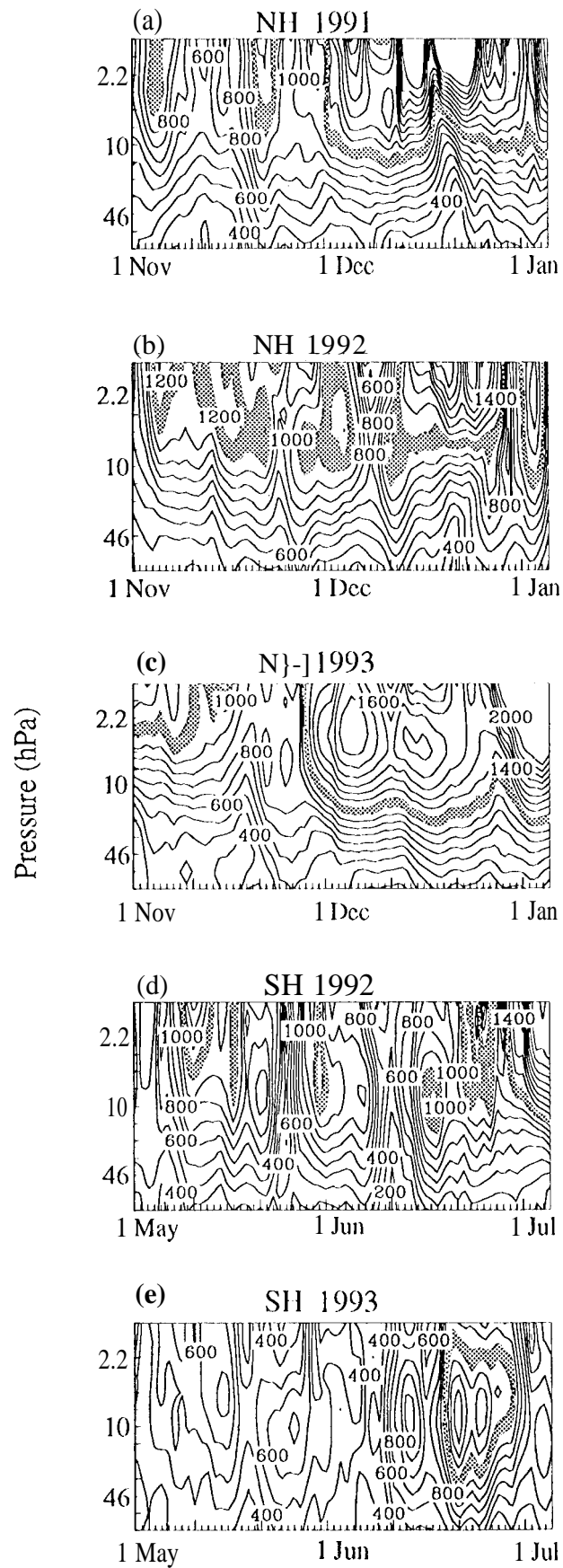


Fig. 2

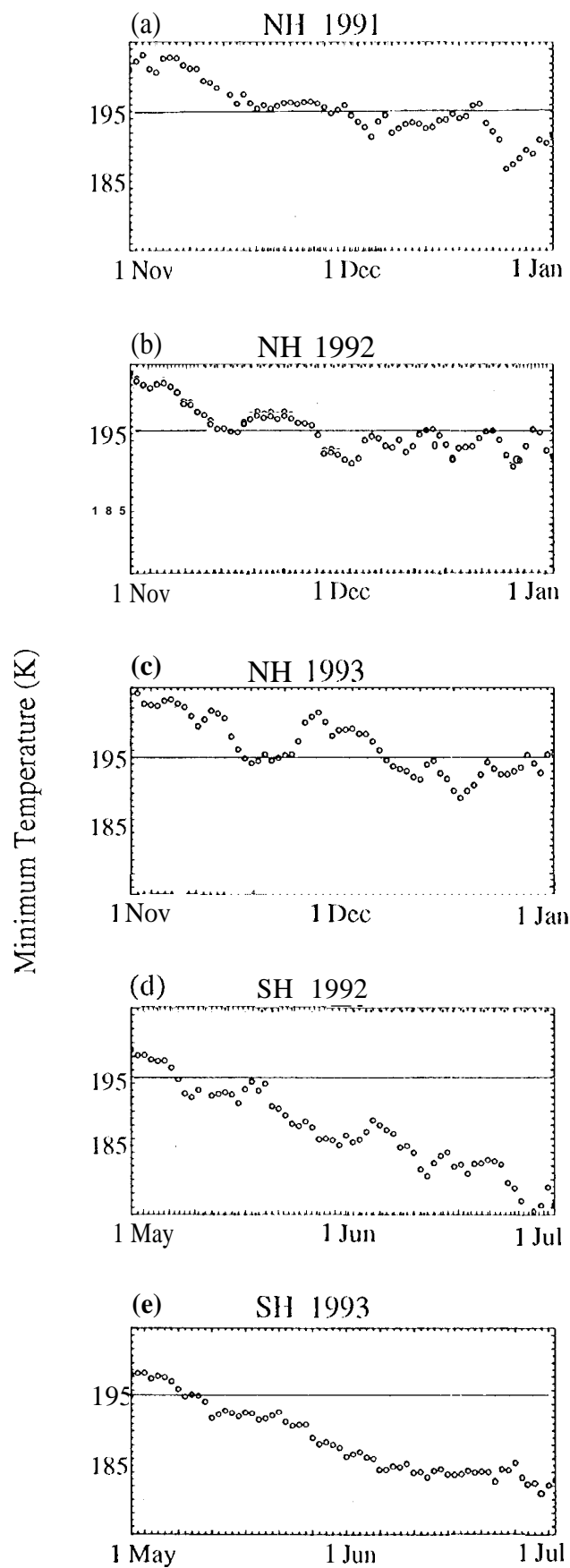


Fig. 3

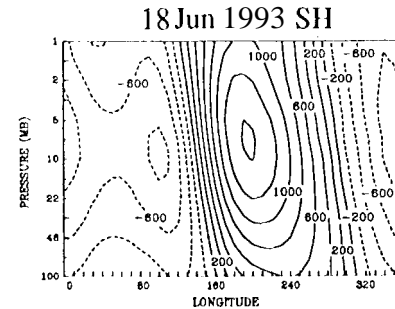
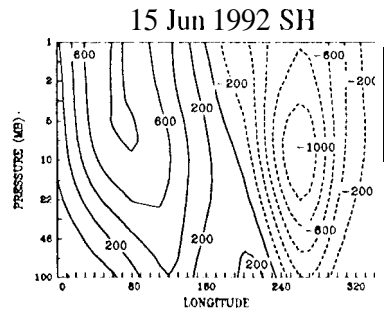
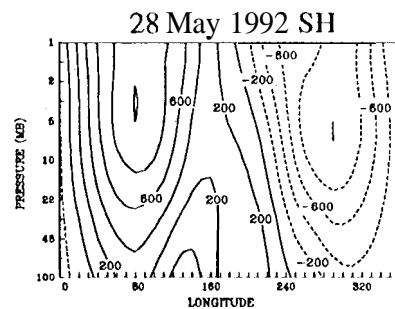
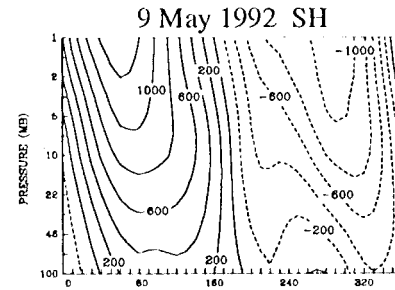
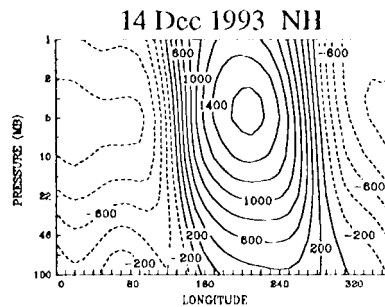
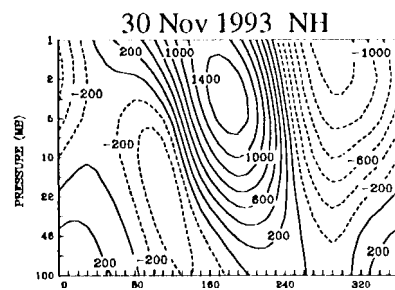
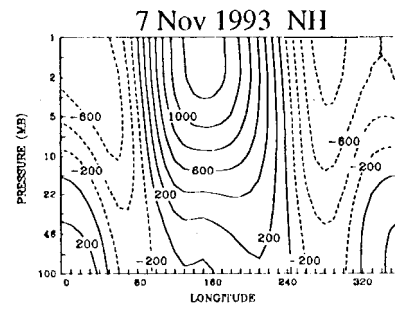
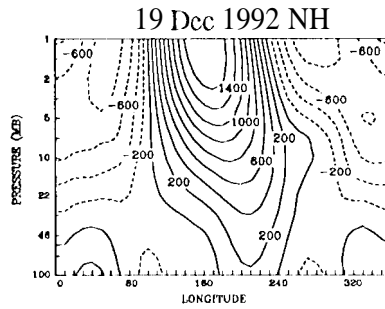
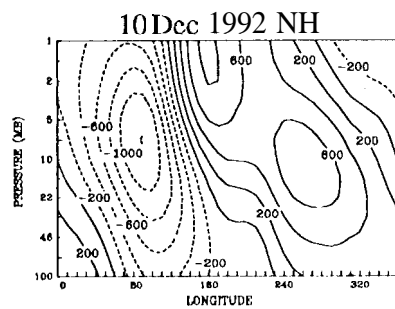
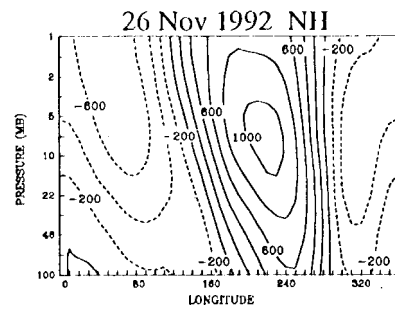
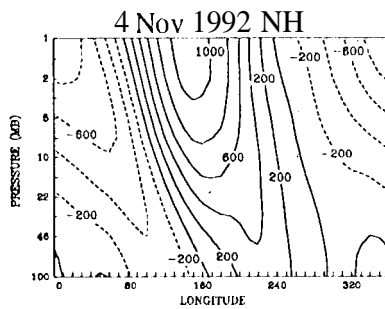
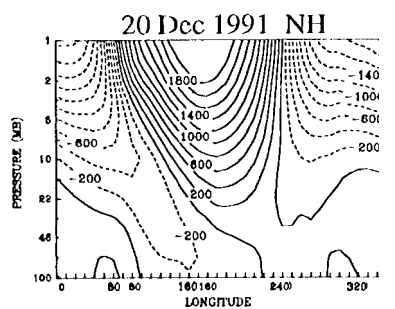
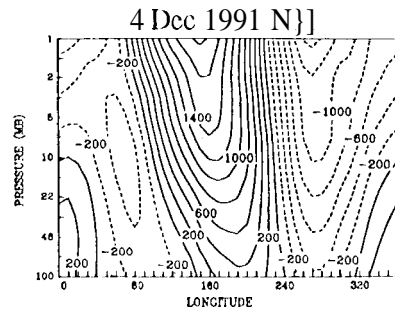
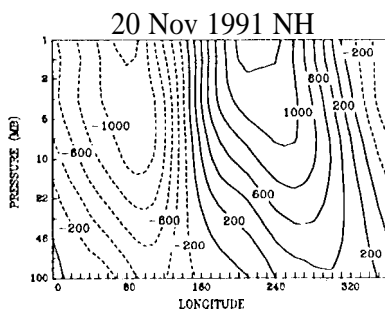
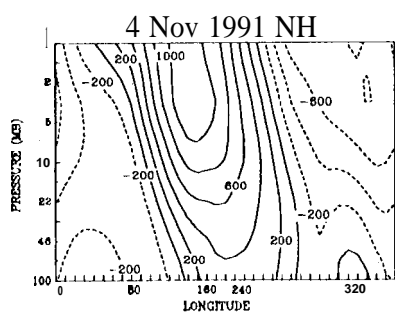


Fig. 4

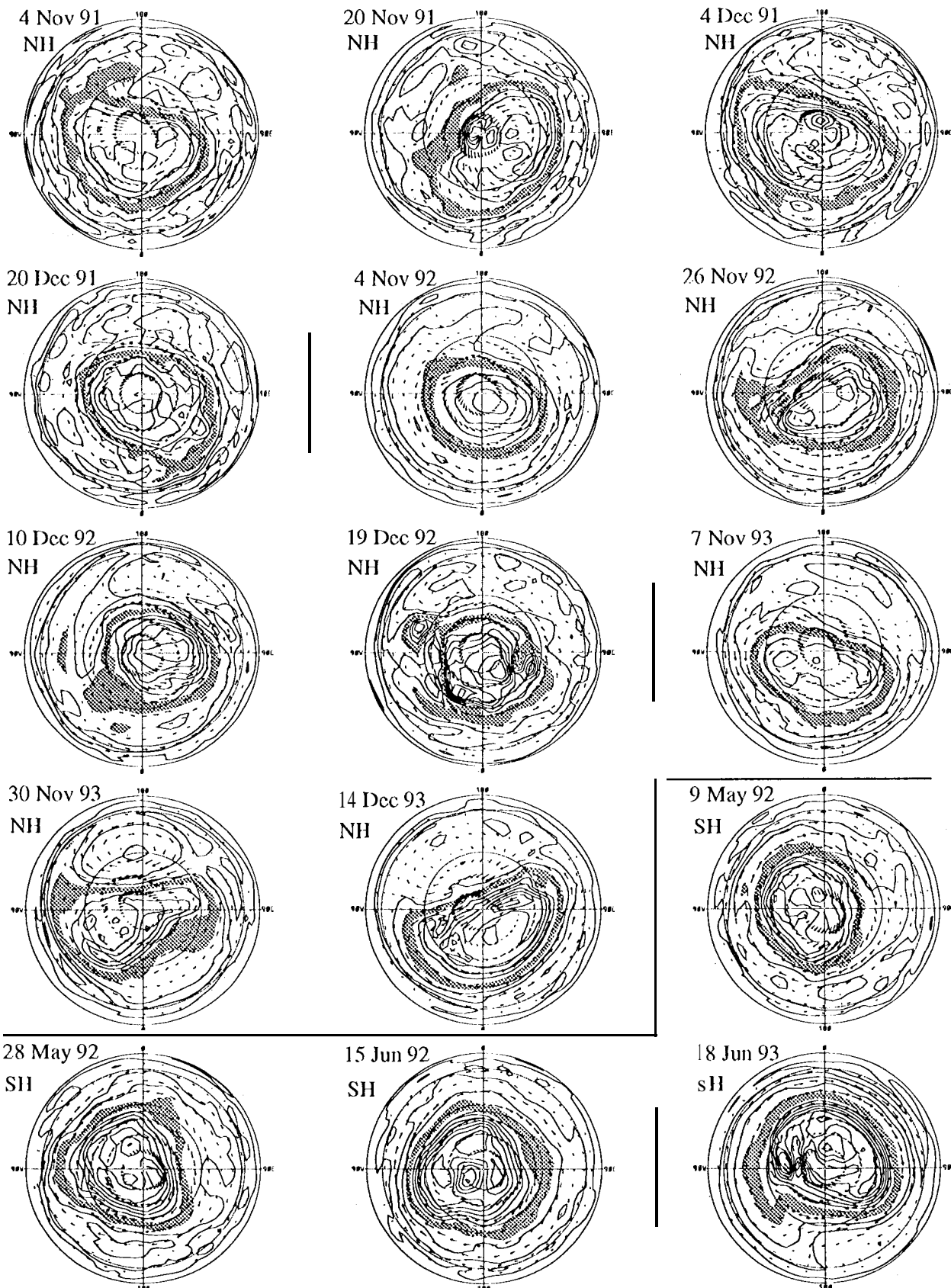
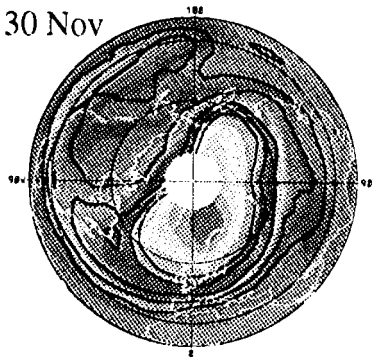


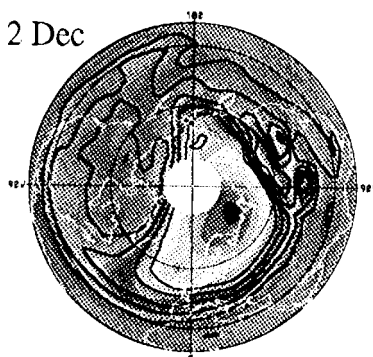
Fig. 5

840 K H₂O (ppmv)NH 1992

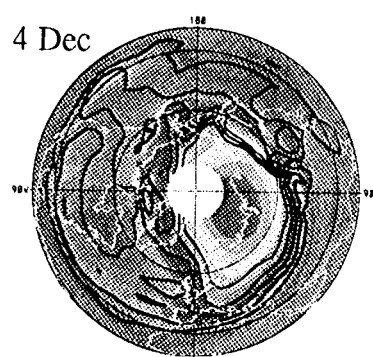
30 Nov



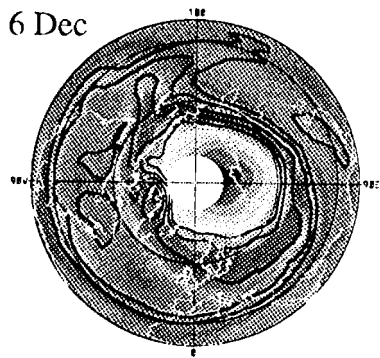
2 Dec



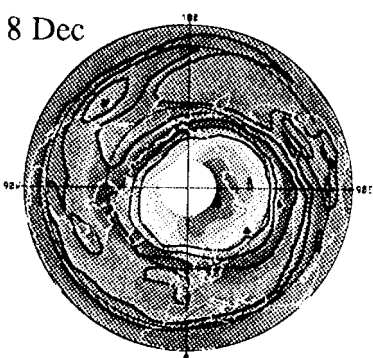
4 Dec



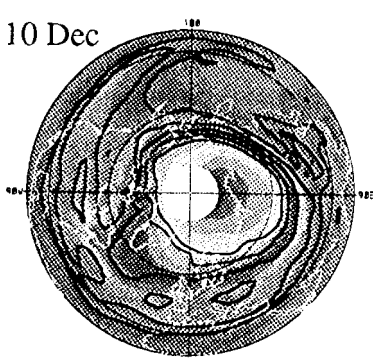
6 Dec



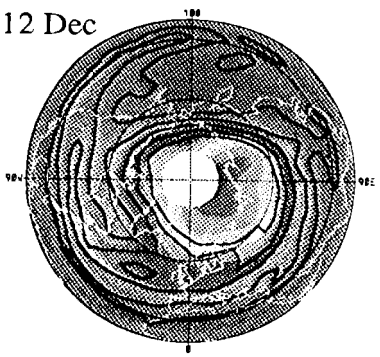
8 Dec



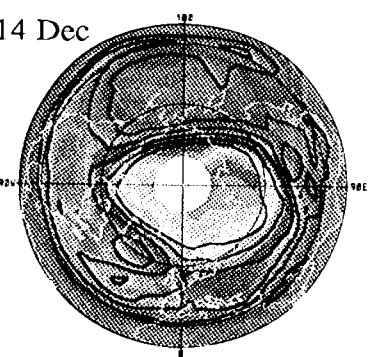
10 Dec



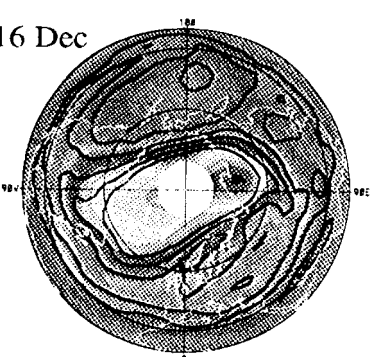
12 Dec



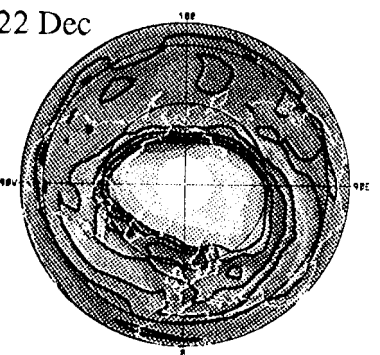
14 Dec



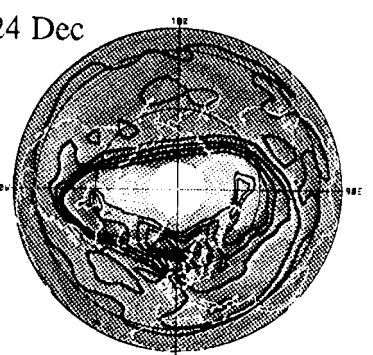
16 Dec



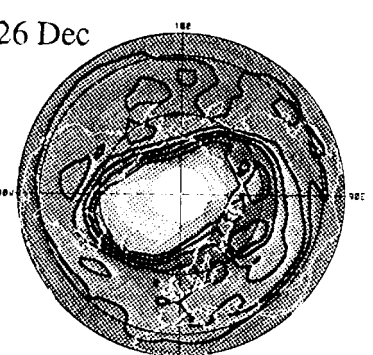
22 Dec



24 Dec



26 Dec



4.5 7.05

Fig. 6

840 K Ozone (ppmv) NH 1992

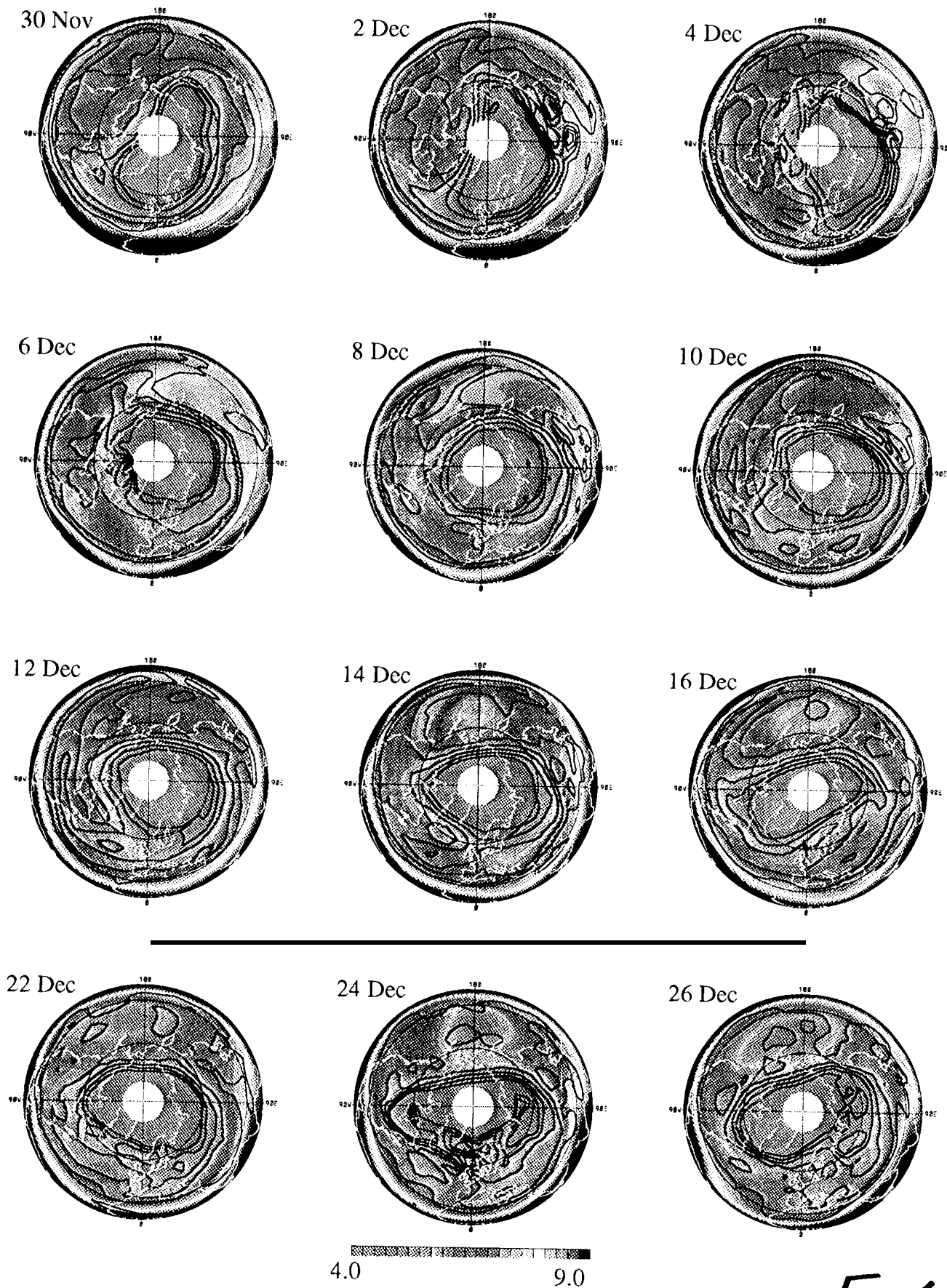


Fig. 6

840 K Ozone (ppmv) NH 1993

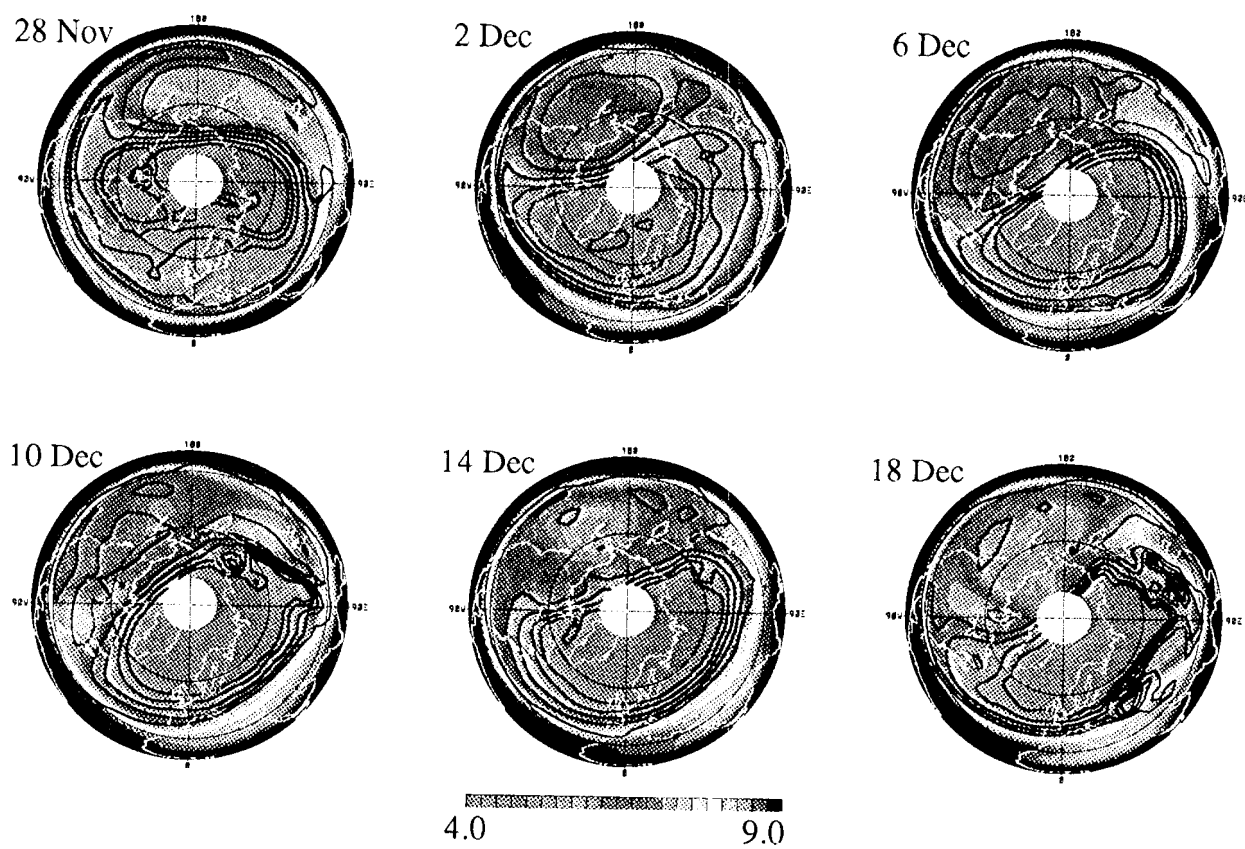


Fig. 7

840 K Ozone (ppmv) SH 1993

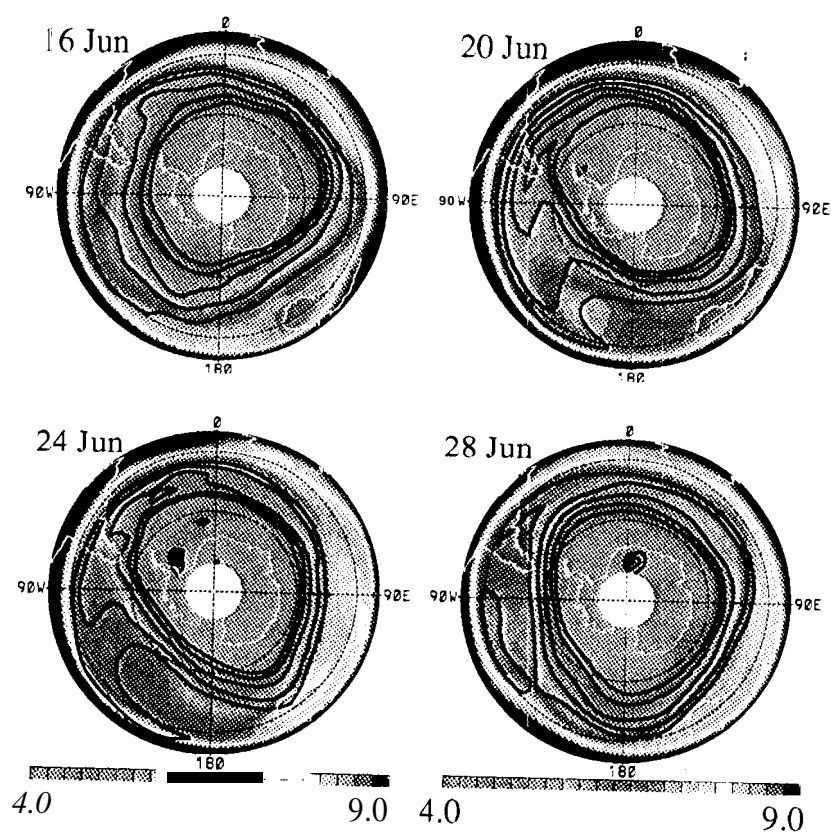


Fig. 8

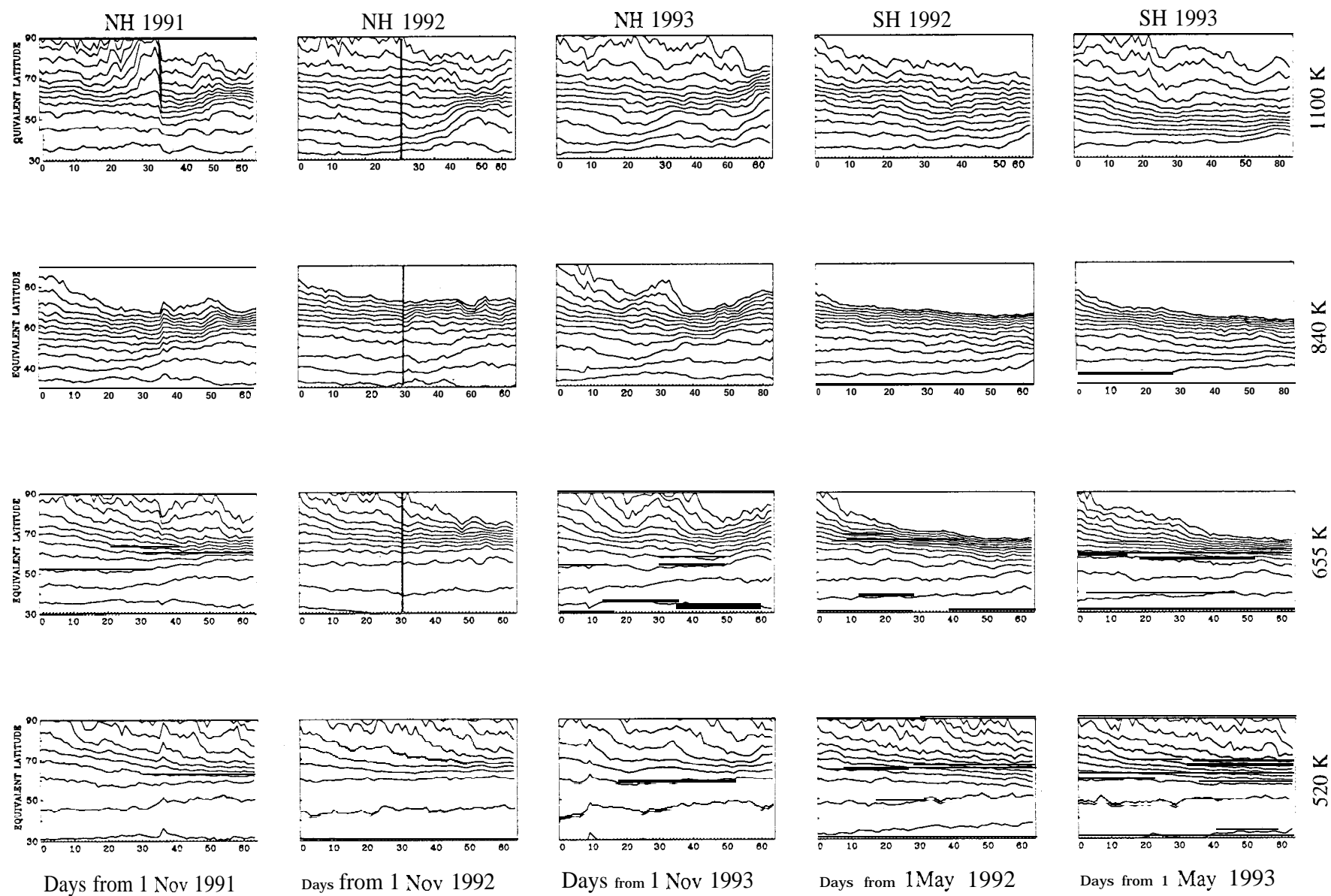
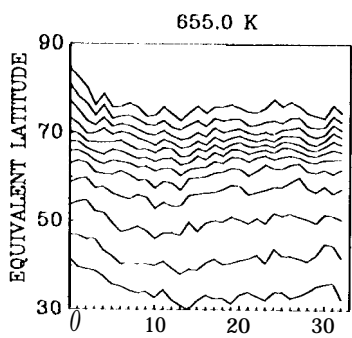
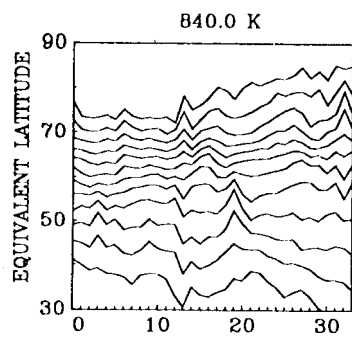
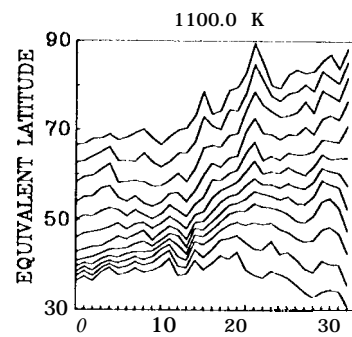


Fig. 9



Days from 30 Nov 1992

Fig 10

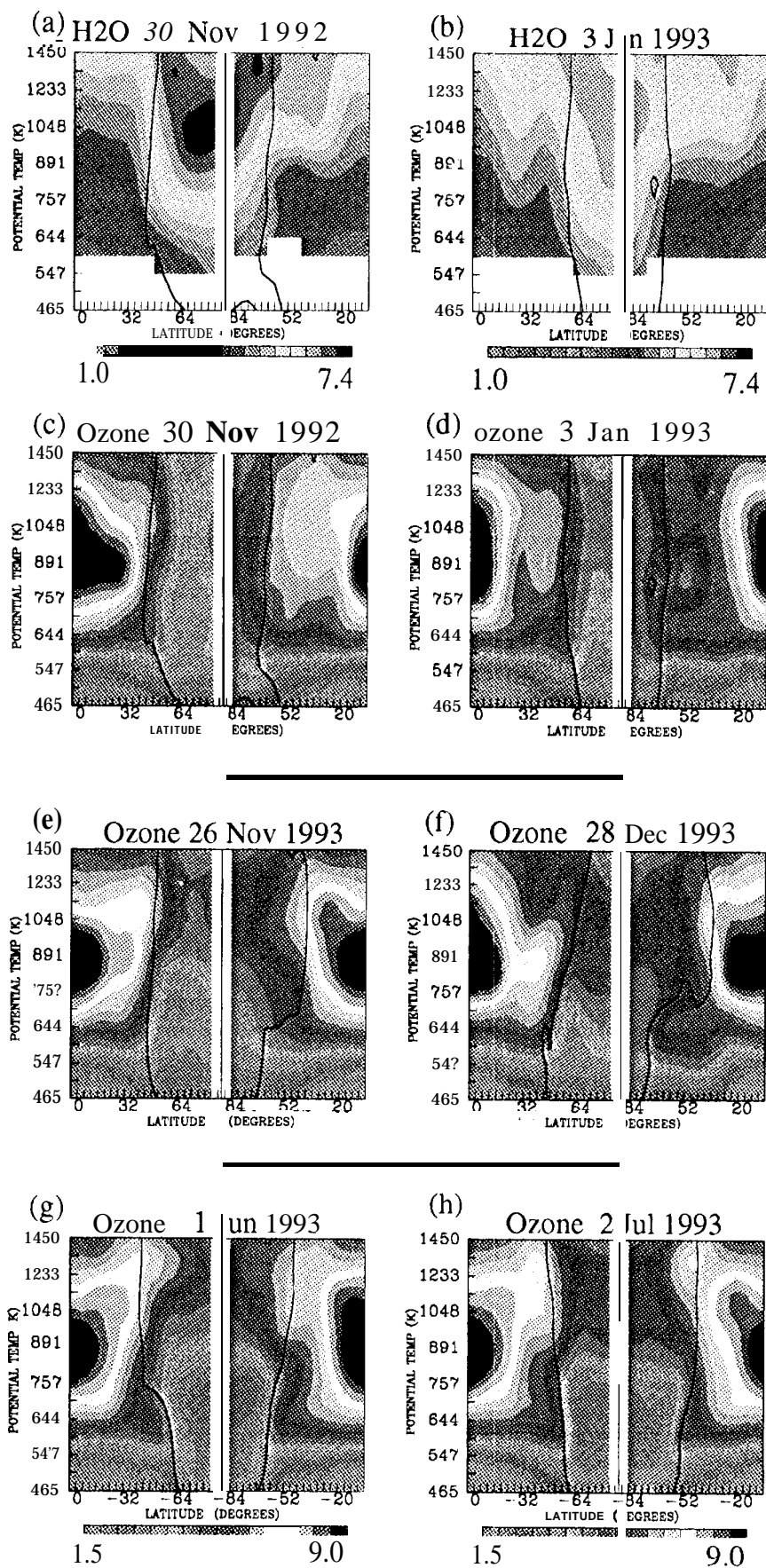


Fig. 11